From feather to fur: gull and mink H5N1 clade 2.3.4.4b HPAIV in their original hosts and their spillover and spillback potential

Albert Perlas Puente
perlasalbert@gmail.com

Helmholtz Munich https://orcid.org/0000-0002-4035-2436

Ferran Tarrés-Freixas
Irta Cresa

Pierre Bessière
IHAP, Université de Toulouse, INRAE, ENVT https://orcid.org/0000-0001-5657-0027

Nicolas Gaide
IHAP, Université de Toulouse, INRAE, ENVT

Laura Martín
IRTA-CReSA

Estefanía Contreras
IRTA-CReSA

Jaume Martorell
IRTA-CReSA

Miquel Nofrarías
IRTA-CReSA

Rosa Valle
IRTA-CReSA

Adrià Girbau
IRTA-CReSA

Marta Pérez
IRTA-CReSA

Mónica Pérez
IRTA, Centre de Recerca en Sanitat Animal (CReSA, IRTA-UAB)

María J. Valdez-May
IRTA-CReSA

Tim Reska
Helmholtz Munich

Iván Cordón

IRTA-CReSA
Natàlia Majó
IRTA-CReSA
Jean-Luc Guérin
IHAP, Université de Toulouse, INRAE, ENVT
Lara Urban
Helmholtz Munich https://orcid.org/0000-0002-5445-9314
Kateri Bertran
IRTA-CReSA

Article

Keywords:

Posted Date: August 14th, 2025

DOI: https://doi.org/10.21203/rs.3.rs-7357485/v1

Additional Declarations: There is **NO** Competing Interest.

From feather to fur: gull and mink H5N1 clade 2.3.4.4b HPAIV in their original hosts and their spillover and spillback potential

Albert Perlas[1,2,#,*], Ferran Tarrés-Freixas[3,4,5,#,*], Pierre Bessière[6], Nicolas Gaide[6], Laura Martín[3,4], Estefanía Contreras[3,4], Jaume Martorell[7], Miquel Nofrarías[3,4], Rosa Valle[3,4], Adrià Girbau[3,4], Marta Pérez[3,4], Mónica Pérez[3,4], María J. Valdez-May[3,4], Tim Reska[1,2,8], Iván Cordón[3,4], Natàlia Majó[4,9], Jean-Luc Guérin[6,$], Lara Urban[1,2,8,10,$], Kateri Bertran[3,4,$,*]

[1] Helmholtz AI, Helmholtz Zentrum München, 85764 Neuherberg, Germany

[2] Helmholtz Pioneer Campus, Helmholtz Zentrum München, 85764 Neuherberg, Germany

[3] Unitat Mixta d'Investigació IRTA-UAB en Sanitat Animal, Centre de Recerca en Sanitat Animal (CReSA), Campus de la Universitat Autònoma de Barcelona (UAB), 08193 Bellaterra, Barcelona, Catalonia, Spain

[4] IRTA Programa de Sanitat Animal, Centre de Recerca en Sanitat Animal (CReSA), Campus de la Universitat Autònoma de Barcelona (UAB), 08193 Bellaterra, Barcelona, Catalonia, Spain

[5] Department of Biosciences, Faculty of Sciences, Technology and Engineering, University of Vic-Central University of Catalonia (UVic-UCC), Vic 08500, Spain

[6] IHAP, Université de Toulouse, INRAE, ENVT, Toulouse, France

[7] Fundació Hospital Clínic Veterinari, Facultat de Veterinària, Universitat Autònoma de Barcelona, Cerdanyola del Vallès 08193, Spain; Departament de Medicina i Cirurgia

Animals, Facultat de Veterinària, Universitat Autònoma de Barcelona, Cerdanyola del Vallès 08193, Spain

[8] Technical University of Munich, School of Life Sciences, 85354 Freising, Germany

[9] Departament de Sanitat i Anatomia Animals, Facultat de Veterinària, Universitat Autònoma de Barcelona (UAB), 08123 Barcelona, Catalunya, Spain

[10] Institute for Food Safety and Hygiene, Vetsuisse Faculty, University of Zurich, CH-8057 Zurich, Switzerland

[#] These authors contributed equally to this work: Albert Perlas and Ferran Tarrés-Freixas.

[$] These authors jointly supervised this work: Jean-Luc Guérin, Lara Urban and Kateri Bertran.

* Correspondence and requests for materials should be addressed to A.P. (perlasalbert@gmail.com), F.T.-F. (ferran.tarres@irta.cat) or K.B. (kateri.bertran@irta.cat).

Abstract

The ongoing panzootic of H5N1 clade 2.3.4.4b high pathogenicity avian influenza virus (HPAIV) increasingly involves non-traditional hosts such as seabirds and mammals. To assess their role in viral-host dynamics and cross-species transmission, we conducted experimental infections in yellow-legged gulls (*Larus michahellis*) and American minks (*Neogale vison*) using HPAIV strains isolated from gulls (H5N1/gull) and minks (H5N1/mink). Infections of gulls with H5N1/gull and minks with H5N1/mink caused viral shedding and high mortality, respectively, and efficient viral transmission from gulls before they developed clinical symptoms. While there was no evidence for H5N1/mink infecting gulls, H5N1/gull subclinically infected minks, followed by neurotropism with a spontaneous emergence of a key mammalian adaptation mutation in the brain, which demonstrates that H5N1 clade 2.3.4.4b spillover events from gulls to minks can lead to fast mammalian adaptation.

Main

Influenza A viruses threaten both human and animal health. Among them, avian influenza viruses (AIVs) are especially concerning since they circulate widely in wild birds and cause outbreaks in poultry farms as well as livestock and wild mammals[1]. Wild waterfowl and shorebirds are reservoirs of low pathogenicity AIVs (LPAIVs)[2] and carry these viruses asymptomatically along migratory routes[3]. In gallinaceous birds, LPAIVs may cause mild illness but can mutate into high pathogenicity AIVs (HPAIVs), increasing mortality and threatening the poultry sector and public health[4].

The hemagglutinin (HA) protein is the primary HPAIV virulence determinant, with subtypes H5 and H7 capable of evolving from LPAIVs into HPAIVs[5]. Since the emergence of the H5Nx Goose/Guangdong (Gs/GD) lineage in 1996 and its intercontinental spread in 2005, outbreaks in poultry and wild birds have surged[6,7] with increasing spillover to mammalian species, including humans[8,9]. The 2016 emergence of H5Nx clade 2.3.4.4b HPAIV and its ecological shifts since 2020 have driven an unprecedented panzootic[10], marked by year-round circulation, broader host range, rapid reassortment, and long-distance spread[11–14]. Within clade 2.3.4.4b HPAIVs, genotype EA-2022-BB has been associated with this expanding host range and the extant circulation in colony-breeding seabirds, which has led to mass mortality events in *Laridae* populations since summer of 2022[15,16].

This panzootic has further led to spillover events in wild mammals[12], infections in domestic cats via hunting and consumption of infected raw by-products [17], outbreaks in fur farms connected to H5N1 HPAIV circulation in gulls (i.e., raccoon dogs, foxes, and minks)[18], and dairy cows infected with genotypes B3.13 and D1.1 in the US[19]. The unchecked circulation of the EA-2022-BB genotype in Europe has led to concerning transmission chains, such as the one reported in a mink farm in Spain in October 2022[16]. As viruses detected in these mammalian species presented key adaptive mutations, these outbreaks have increased the risk of spillover events to humans with potential human-to-human transmission[20]; by June 2025, an increased number of human H5N1 HPAIV infections, usually linked to contact with infected animals, has been reported[21].

Despite ongoing surveillance, the expanding host range and the potential new role of colony-breeding seabirds as reservoirs of H5N1 HPAIV warrant new assessments of the viral-host dynamics and transmission mechanisms in seabirds and mammals. Previous experimental infections in gulls suggested that H5Nx Gs/GD-related HPAIV strains belonging to clades 2.2[22] and 2.3.4.4b[23] poorly transmit among individuals. Similarly, one of the few experimental infections in minks suggested that H7N9, H5N6, and H9N2 AIVs are not capable of aerosol transmission[24]. Furthermore, ferret transmission experiments with H5N1 clade 2.3.4.4b HPAIV isolated from minks were inconsistent, ranging from no infection[25] to moderate aerosol transmission[20]. The viral-host dynamics of H5N1 clade 2.3.4.4b HPAIVs and especially its EA-2022-BB genotype, as well as its cross-species transmission mechanisms in novel hosts such as mammals and colony-bredding seabirds are therefore poorly understood. Here, we report experimental infections in yellow-legged gulls (*Larus michahellis*) and American minks (*Neogale vison)* using two H5N1 clade 2.3.4.4b Gs/GD-related HPAIV strains from the EA-2022-BB genotype, one isolated from the mink farm outbreak in Spain in October 2022, and another one isolated from a gull in Spain during the same season. We leveraged this experimental setup to evaluate viral-host dynamics and transmission of H5N1 HPAIV in these *in vivo* models for seabirds and mammals, and to assess the potential for spillover and spillback events in nature.

Results

Experimental infection in gulls

Clinical signs and mortality in gulls

Animals were challenged with one H5N1 HPAIV strain isolated from gulls (H5N1/gull) or one from minks (H5N1/mink); for each challenge virus, 10 gulls were inoculated, four gulls were used as direct contacts, and four gulls as aerosol contacts**.** Gulls inoculated with H5N1/gull started showing clinical signs at 6 days post-inoculation (dpi), including listlessness, incoordination, dyspnea, head tremors, ruffled feathers, antalgic posture, and cloacal soiling and reached humane endpoint (HEP) criteria before the experimental endpoint (Figure 1a; left). Three of the four direct contact gulls showed clinical signs akin to the inoculated gulls and were euthanised between 7 and 12 dpi (Figure 1a; left). All aerosol contacts showed mild listlessness from 9 dpi onwards; while two of them survived until the end of the study, the other two progressed to severe clinical disease. No seroconversion was observed in any aerosol contact (10-14 dpi) (Figure 1b; left), suggesting that their clinical manifestations were probably due to unrelated causes. Overall, we observed 100% mortality and a mean death time (MDT) of 9 days for the inoculated gulls, 75% mortality and a MDT of 10 days for the direct contact gulls, and 0% mortality for the aerosol contact gulls (Figure 1a; left). All but one inoculated gull had seroconverted by the time of euthanasia (6-13 dpi). All three direct contact gulls that were ethically euthanised had seroconverted by the time of euthanasia (7-12 dpi), as did the contact gull that survived (14 dpi) (Figure 1b; left).

In contrast, no clinical signs, mortality (Figure 1a; right), or seroconversion (Figure 1b; right) were observed in the inoculated and contact gulls of the H5N1/mink experimental room.

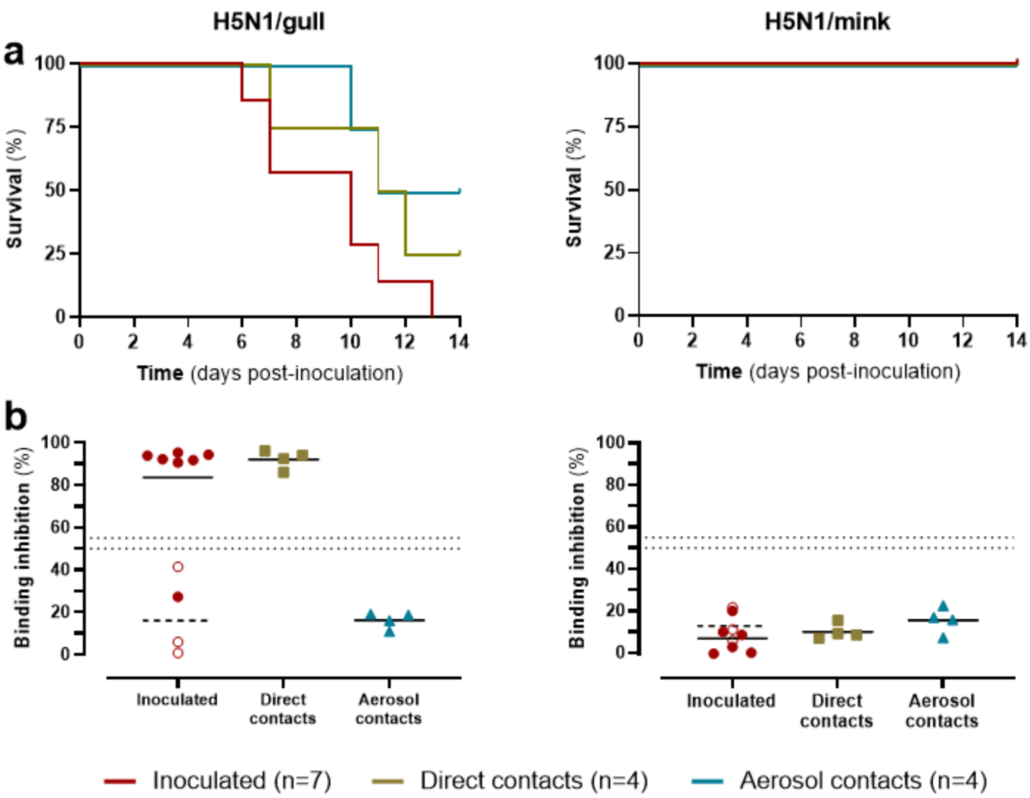

Figure 1. Percentage of survival and seroconversion of gulls experimentally infected with A/Larus ridibundus/Spain/CR4063/2023 (H5N1/gull, left) or A/Mink/Spain/3691-8_22VIR10586-10/2022 (H5N1/mink, right). **a,** Kaplan-Meier survival curve for gulls experimentally infected with H5N1/gull (left; two out of four H5N1/gull aerosol contacts were euthanised due to unrelated causes) and H5N1/mink (right). **b,** Detection of anti-nucleoprotein antibodies in serum of H5N1/gull (left) and H5N1/mink (right) groups. Data presented as individual values; empty symbols represent animals euthanised at 3 dpi (n=3) with their mean in dashed lines, while solid symbols represent animals euthanised at endpoint (experimental or humane) with their mean in solid lines. Dotted lines represent positivity thresholds.

Viral RNA detection in gull samples and environmental samples

To investigate viral shedding, oropharyngeal swabs, cloacal swabs, and feather pulp samples were collected at different time points. Inoculated and direct contacts in the H5N1/gull experimental room showed oropharyngeal and cloacal viral shedding between 4 and 10 dpi, with peak viral titers between 7 and 10 dpi (Figure 2a-b). Mean viral RNA levels in oropharyngeal swabs were higher than those in cloacal swabs of inoculated gulls at all time points, with a significant difference at 10 dpi. Direct contact gulls showed a viral shedding pattern similar to inoculated gulls with a 5-day delay, with the only surviving direct contact also being PCR-positive in all 14 dpi swabs. Mean viral RNA levels between inoculated and direct contact gulls were not statistically different when comparing each group and day. Viral RNA in feather pulp samples mirrored the oropharyngeal and cloacal swab results (Figure 2c). Viral RNA in blood was confirmed starting at 6 dpi in inoculated gulls and at 7 dpi in direct contacts, and viremia lasted until 10-11 dpi (Figure 2d). No viral RNA was detected in any aerosol contact gull at any time point.

At necropsy, tissues were also collected for viral RNA quantification by RT-qPCR. Brain, lung, spleen, and heart were collected from three inoculated gulls at 3 dpi, and from up to three gulls per condition (inoculated, direct contacts, and aerosol contacts). High quantities of viral RNA were detected in all the tissues from H5N1/gull-inoculated and direct contact gulls (Figure 2e). Mean viral RNA levels were not significantly different between inoculated and direct contact gulls. The brain had the highest amount of virus, followed by the lung, heart, and spleen. Mean viral RNA levels in the brain were significantly higher than those in the spleen. No viral RNA was detected in any tissue from asymptomatic H5N1/gull inoculated gulls necropsied at 3 dpi, or from aerosol contact gulls.

To evaluate viral contamination in the environment, aerosol and drinking water samples were collected. In the H5N1/gull experimental room, viral RNA was detected in the active air sampler between 3 and 10 dpi at increasing levels (Figure 2f). In contrast, the passive air sampler yielded only one positive sample at 7 dpi. Viral RNA was detected in drinking water samples of the H5N1/gull experimental room throughout the study.

Neither viral shedding nor viral RNA in environmental samples was detected in the H5N1/mink experimental room.

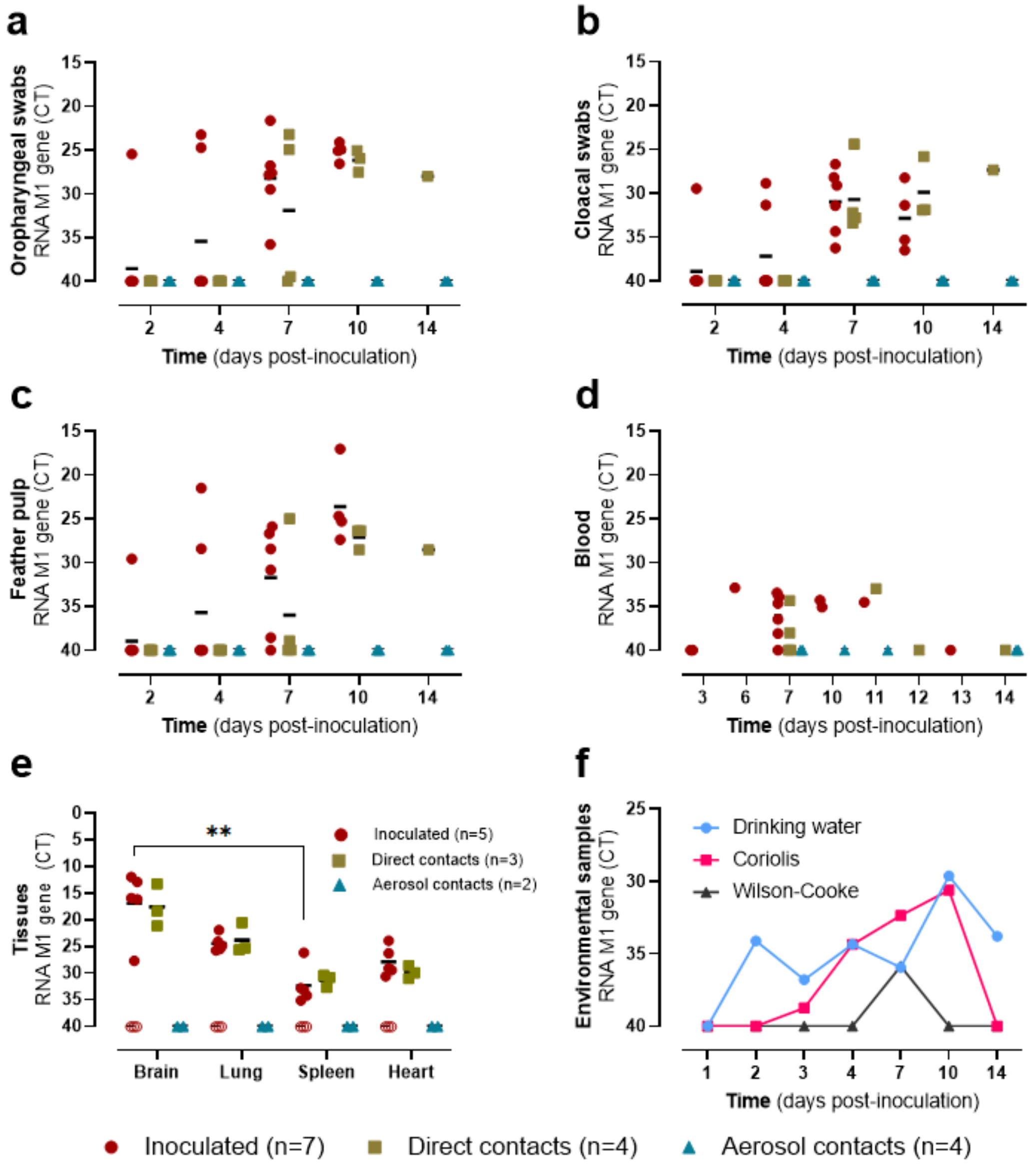

Figure 2. Viral RNA detection in samples from gulls experimentally infected with A/Larus ridibundus/Spain/CR4063/2023 H5N1 HPAIV. Black lines represent the mean of each group per timepoint. **a,** Oropharyngeal swabs. **b,** Cloacal swabs. **c,** Feather pulp samples. **d,** Viremia. **e,** Tissues collected from gulls at endpoint. Data presented as individual values; empty symbols represent animals euthanised at 3 dpi (n=3) with their mean in dashed lines, while solid symbols represent animals euthanised at endpoint (experimental or humane) with their mean in solid lines. Statistically significant differences were found between tissues using a Kruskal-Wallis test with Dunn's correction for multiple comparison (***p*<0.005). **f,** Aerosol samples using the active Coriolis µ Air sampler (magenta) and the passive Modified Wilson and Cooke sampler (grey). Drinking water samples (blue).

Necropsy findings in gulls

Three inoculated gulls per virus were euthanised and necropsied at 3 dpi to evaluate pathobiological changes in the asymptomatic phase, while up to three clinically-affected gulls per virus and condition were necropsied throughout the experiment. At necropsy, gross findings were observed in H5N1/gull inoculated gulls (6, 7 and 10 dpi) and in H5N1/gull direct contact gulls (7-12 dpi). Gross findings included diffuse pulmonary congestion, splenic enlargement and congestion, mottled pancreas, and meningeal congestion. Negative controls, H5N1/mink inoculated and contact gulls, and H5N1/gull inoculated gulls at 3 dpi were within normal limits.

Histopathology and viral detection in gull tissues

At 3 dpi, most tissues from gulls inoculated with H5N1/gull virus appeared within normal limits, and mild changes were only observed in the nasal cavity and lungs, including mucosal epithelial attenuation and mild infiltration by heterophilic and mononuclear leukocytes. In clinically affected gulls inoculated with H5N1/gull and euthanised between 6 and 10 dpi, moderate-to-severe necrotizing and non-suppurative lesions were observed, primarily in the brain, nasal cavity, and pancreas, with milder involvement of the lungs, liver, and heart. Similar lesions were found in direct contact birds. No relevant findings were observed in negative controls, aerosol contacts, or gulls inoculated with H5N1/mink. Brain, lung, spleen, and heart were also collected for virological analyses. Viral antigen detection was negative in H5N1/gull inoculated birds necropsied during the acute phase (3 dpi) and in H5N1/gull aerosol contacts. In clinically affected inoculated and direct contact H5N1/gull birds, viral antigen was consistently detected in the brain, pancreas, and lung, more sporadically in the nasal cavity, and rarely in the liver and heart. Antigen-positive cells included neurons, glial and ependymal cells in the brain, epithelial cells in respiratory and digestive tissues, and cardiomyocytes. No viral antigen was detected in tissues from the negative controls, inoculated, and contact gulls of the H5N1/mink experiment.

Nanopore genomics in gull samples

Three oropharyngeal swabs from RT-qPCR-positive H5N1/gull-inoculated (n=3) and direct contact (n=3) gulls collected at 10 dpi were sequenced to assess viral adaptation and potential transmission-related mutations (Supplementary Table 1). Whole viral genomes were assembled (mean coverage from ~1900 to 5000x). No amino acid substitutions were detected between the viral genomes of the original inoculum, the inoculated and the contact gulls.

Experimental infection in minks

Clinical signs and mortality in minks

For each challenge virus (H5N1/gull and H5N1/mink), seven minks were inoculated (three were euthanised at 3 dpi), two minks were used as direct contacts, and six minks as aerosol contacts. All H5N1/mink-inoculated minks started showing weight loss and increased rectal temperature between 2 and 4 dpi (Figure 3a-b; left). These animals reached HEP between 5 and 7 dpi (Figure 3c; left). None of the direct contacts nor aerosol contacts displayed clinical signs (Figure 3a-b; left), except for one female aerosol contact that had started experiencing significant weight loss already before the experimental challenge (Figure 3a; left). None of the contact animals were euthanised throughout the study (14 days), except for one male direct contact that was euthanised for reasons unrelated to the study (Figure 3c; left).

H5N1/gull-inoculated or contact minks showed no clinical signs nor mortality (Figure 3a-c; right), except for mink #4 that experienced a notable weight loss from 7 dpi onwards without any other clinical sign nor temperature variation (Figure 3a, right; red arrow). Despite this significant weight loss, mink #4 survived until the experimental endpoint.

H5N1/gull-inoculated minks seroconverted from 7 dpi onwards (Figure 3d). None of the contact animals seroconverted.

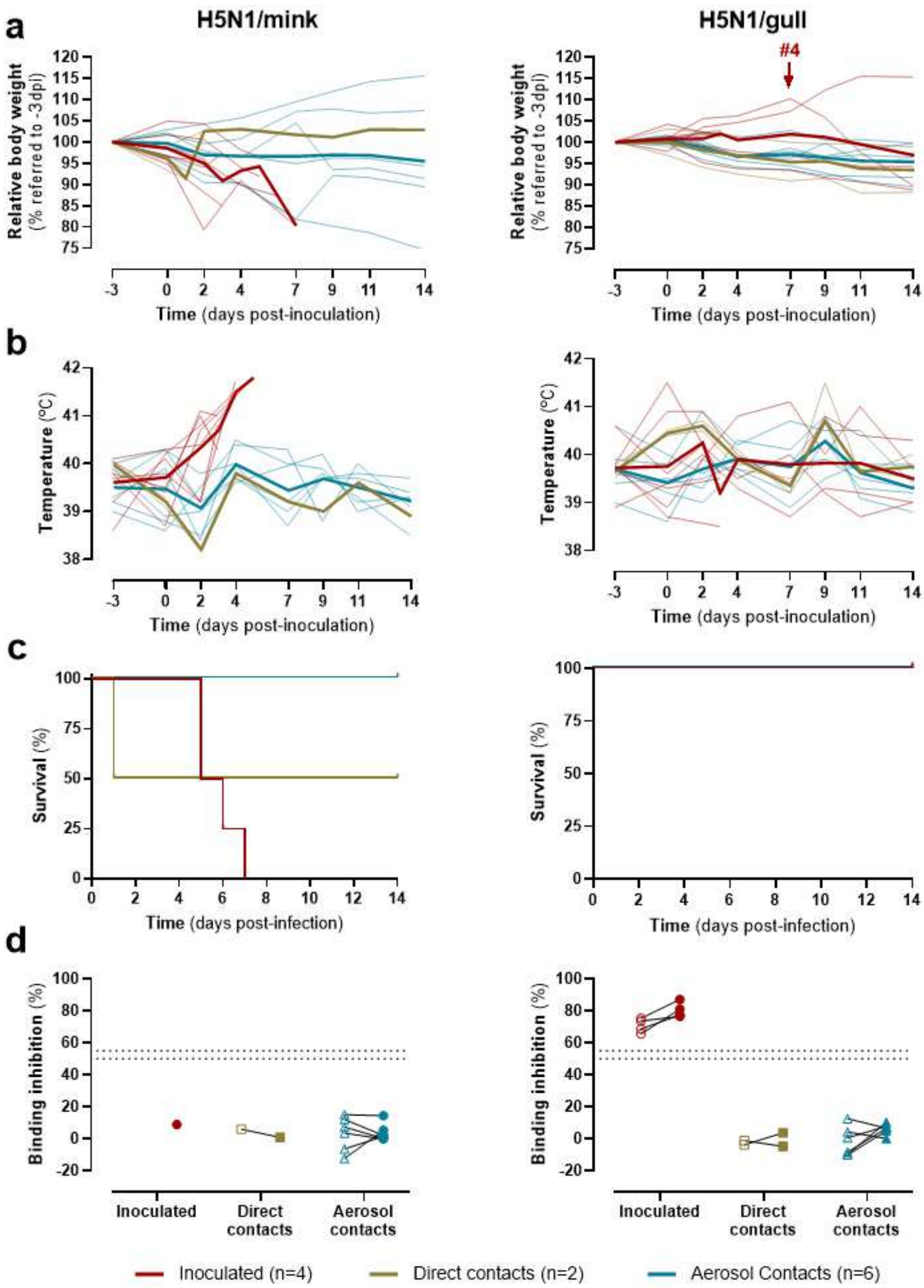

Figure 3. Clinical signs, percentage of survival, and seroconversion in minks experimentally infected with A/Mink/Spain/3691-8_22VIR10586-10/2022 (H5N1/mink, left) or A/Larus ridibundus/Spain/CR4063/2023 (H5N1/gull, right) H5N1 HPAIV. **a,** Body weight variation (relative to -3 dpi). Thick lines represent mean values and thin lines represent individual values. **b,** Rectal temperature variation. Thick lines represent mean values and thin lines represent individual values. **c,** Kaplan-Meier

survival curve. **d,** Detection of anti-nucleoprotein antibodies in serum. Dotted lines represent the positivity threshold. Empty symbols represent samples collected at 7 dpi, while solid symbols represent samples collected at humane or experimental endpoints. Experimental endpoint is 14 dpi for H5N1/mink and 16 dpi for H5N1/gull.

H5N1/mink-inoculated minks presented a more pronounced mean weight loss than H5N1/gull-inoculated minks (Figure 3b and Supplementary Figure 3a-d), which was significant at endpoint (Supplementary Figure 3d, $p<0.05$). Mean rectal temperature of the H5N1/mink-inoculated minks increased over time, and the last measured temperature (4 dpi) was significantly higher than the temperature of H5N1/gull-inoculated minks (Figure 3a and Supplementary Figure 3e-h). The appearance of clinical signs correlated with animals reaching HEP (Supplementary Figure 3i).

Viral RNA detection in mink and environmental samples

To evaluate viral shedding, oropharyngeal swabs were collected at different time points. H5N1/mink-inoculated minks had higher viral RNA levels at all time points than H5N1/gull-inoculated minks (Figure 4a; Supplementary Figure 3j-k). No viral RNA was detected in the oropharyngeal swabs from any direct or aerosol contact, except for one direct contact of H5N1/gull-inoculated minks, that yielded viral RNA levels close to the limit of detection at 4 dpi (Figure 4a, right).

Lung, brain, and blood were also collected for virological analyses. Viral RNA detection in these samples followed a similar pattern. All minks inoculated with the H5N1/mink virus had detectable viral RNA in all tissues (Figure 4b; left), with higher viral RNA loads in samples from animals that reached HEP compared to those euthanised at 3 dpi. None of the minks inoculated with the H5N1/gull virus had any detectable viral RNA in the lungs nor blood (Figure 4b; right). Two out of four H5N1/gull-inoculated minks (minks #2 and #4) had detectable viral RNA in the brain at 16 dpi, with no other sign of systemic infection. No viral RNA was detected in any lung or brain sample from direct or aerosol contacts (Figure 4b).

To evaluate viral contamination in the environment, aerosol samples were collected with an active air sampler. No viral RNA was detected in any air sample.

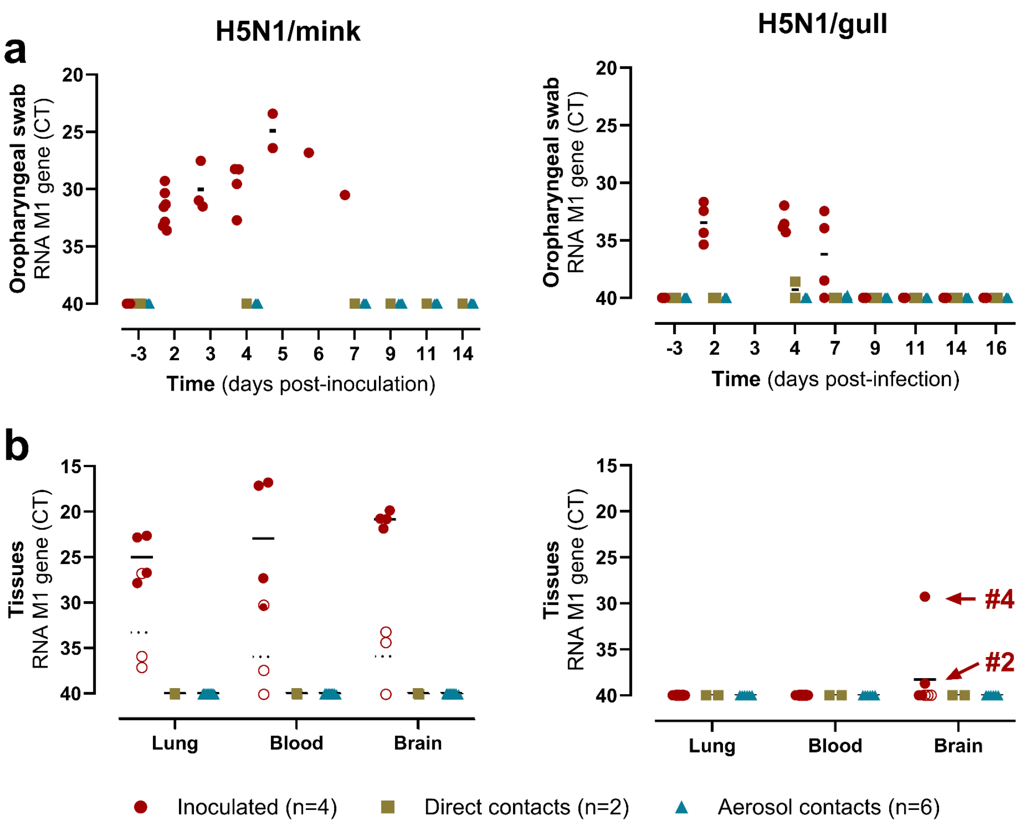

Figure 4. Viral RNA detection in samples from minks experimentally infected with A/Mink/Spain/3691-8_22VIR10586-10/2022 (H5N1/mink, left) or A/Larus ridibundus/Spain/CR4063/2023 (H5N1/gull, right) H5N1 HPAIV. **a,** Oropharyngeal swabs. **b,** Tissue samples collected at necropsy. Data presented as individual values; empty symbols represent animals euthanised at 3 dpi (n=3) with their mean in dashed lines, while solid symbols represent animals euthanised at endpoint (experimental or humane) with their mean in solid lines.

Necropsy findings in minks

At necropsy, negative controls, contact minks and minks inoculated with H5N1/gull showed no gross abnormalities in any tissues (Supplementary Figure 4a-b). H5N1/mink-inoculated minks presented multiple red foci scattered among the lung parenchyma and, to a lesser extent, in the kidney, which is consistent with congestive to hemorrhagic changes (Supplementary Figure 4c-d). The intestine had prominent red hemorrhagic luminal content. The liver appeared diffusely enlarged, friable, and yellow-to-tan (Supplementary Figure 4e). Several of these extrapulmonary lesions were also found in some direct and aerosol contacts of H5N1/mink virus, which could indicate they were unrelated to HPAIV infection, albeit not as frequent or severe as in inoculated animals.

Histopathology and viral detection in mink tissues

Lesions were observed in all minks inoculated with H5N1/mink that had reached HEP (4/4) (Figure 5). They included acute rhinitis (Figure 5a), meningo-encephalitis (Figure 5b), and interstitial pneumonia (Figure 5c). Pneumonia was also observed in one mink inoculated with H5N1/mink at 3 dpi (1/3). Viral antigens were detected in the same individuals and colocalized with lesions. Positive cell types included nasal epithelial cells (Figure 5d), neurons (Figure 5e), alveolar cells (Figure 5f), as well as immune cells, with both nuclear and cytoplasmic staining. No significant lesions or viral antigen detection were found in direct or aerosol contacts, nor in any negative control (Supplementary Table 2).

Lesions in H5N1/gull-inoculated minks were mild, infrequent, and mainly confined to the nasal cavity during early infection (at 3 dpi) or in the lungs at late stages of infection (at 16 dpi). These mild respiratory lesions included rhinitis with epithelial deciliation and attenuation (Figure 5g), interstitial pneumonia, and bronchus-associated lymphoid tissue hyperplasia. Two animals euthanised at experimental endpoint also presented non-suppurative meningoencephalitis (Figure 5h). Viral antigen was detected in the nasal mucosal epithelium (rostral and/or caudal) of two individuals at 3 dpi (Figure 5i). Viral antigen colocalized with lesions in the brain of mink #4, but was not detected in mink #2 (Figure 5j). To improve detection sensitivity, RNAscope in situ hybridization (ISH) was employed in these samples and viral RNA was detected in the brain (frontal lobe and/or temporal and occipital lobes) of minks #2 and #4, respectively, at endpoint (Figure 5k), suggesting limited replication and localized persistence (Supplementary Table 2).

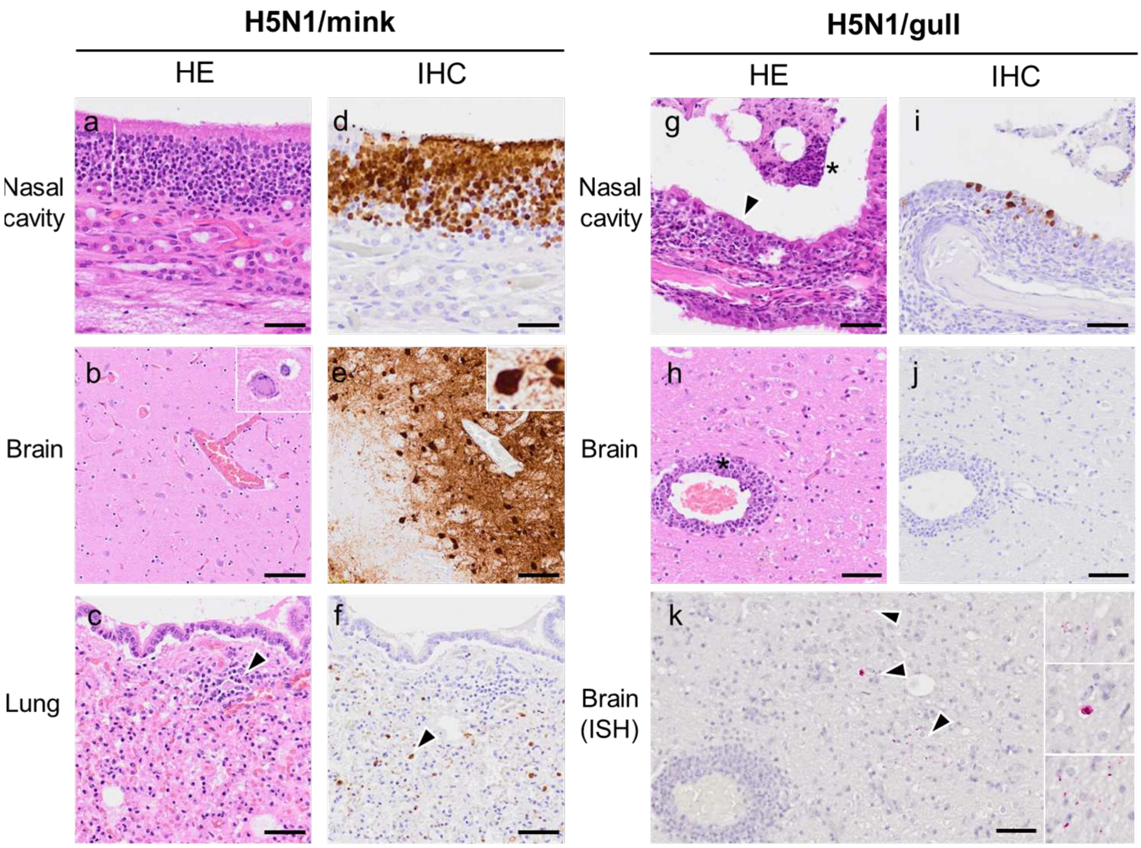

Figure 5. Histopathological findings and viral antigen detection. Tissues of minks experimentally infected with A/Mink/Spain/3691-8_22VIR10586-10/2022 (H5N1/mink) (**a-f**) and A/Larus ridibundus/Spain/CR4063/2023 (H5N1/gull) (**g-k**) H5N1 HPAIVs. **a**, Nasal cavity, olfactory epithelium with discrete nuclear pyknosis. Hematoxylin and eosin (HE), sb=50 µm. **b**, Cerebro-cortex, acute vascular

congestion and neuronal degeneration. HE, sb=100 μm. **c**, Lung, lymphocytic infiltration within pulmonary parenchyma (arrow). HE, sb=50 μm. **d**, Nasal cavity, extensive antigen detection in the olfactory epithelium. Anti-nucleoprotein influenza A immunohistochemistry (IHC), sb=50 μm. **e**, Cerebro-cortex, extensive viral antigen in neurons. IHC, sb=100 μm. **f**, Lung, sparse viral antigen in alveoli (arrow). IHC, sb=50 μm. **g**, Nasal cavity, epithelial attenuation and deciliation (arrow), leucocytic infiltration, and necrotic debris within lumen (asterisk). HE, sb=50 μm. **h**, Cerebro-cortex, lymphocytic infiltration expanding Robin-Virchow spaces (asterisk). HE, sb=100 μm. **i**, Nasal cavity, sparse viral antigen in olfactory mucosa. IHC, sb=50 μm. **j**, Cerebro-cortex, absence of antigen detection. IHC, sb=100 μm. **k**, Cerebro-cortex, sparse viral RNA detection in neurons (arrows). RNAscope in situ hybridization (ISH) targeting avian influenza A matrix protein RNA, sb=100 μm.

Nanopore genomics in mink samples

To assess viral adaptation and potential transmission-related mutations, we sequenced the oropharyngeal swabs (at 7 dpi) and brain samples (at 16 dpi) from the H5N1/gull-inoculated minks #2 and #4 with RT-qPCR-positive brain samples (Supplementary Table 1). Whole viral genomes were assembled from the nanopore sequencing data (mean coverage from 945 to 3842x). Variant calling revealed the emergence of three amino acid substitutions in the brain sample of mink #4 that were not present in the original inoculum nor in the respective oropharyngeal swab: polymerase basic 2 (PB2) T271A, matrix (M) E204K, and HA K293R (Figure 6; Supplementary Table 4). While the brain of mink #2 only showed synonymous mutations, the non-synonymous substitution PB2 S74N was detected in the respective oropharyngeal swab.

We further sequenced three RT-qPCR-positive oropharyngeal swabs that were collected at 4 dpi from H5N1/mink-inoculated minks (mink #19, #20, and #23) (Supplementary Table 1). Whole viral genomes were assembled from the nanopore sequencing data (mean coverage from 984 to 4989x). The oropharyngeal swab of mink #19 showed the PB2 D611N substitution, and the one of mink #23 the PB2 M645L substitution.

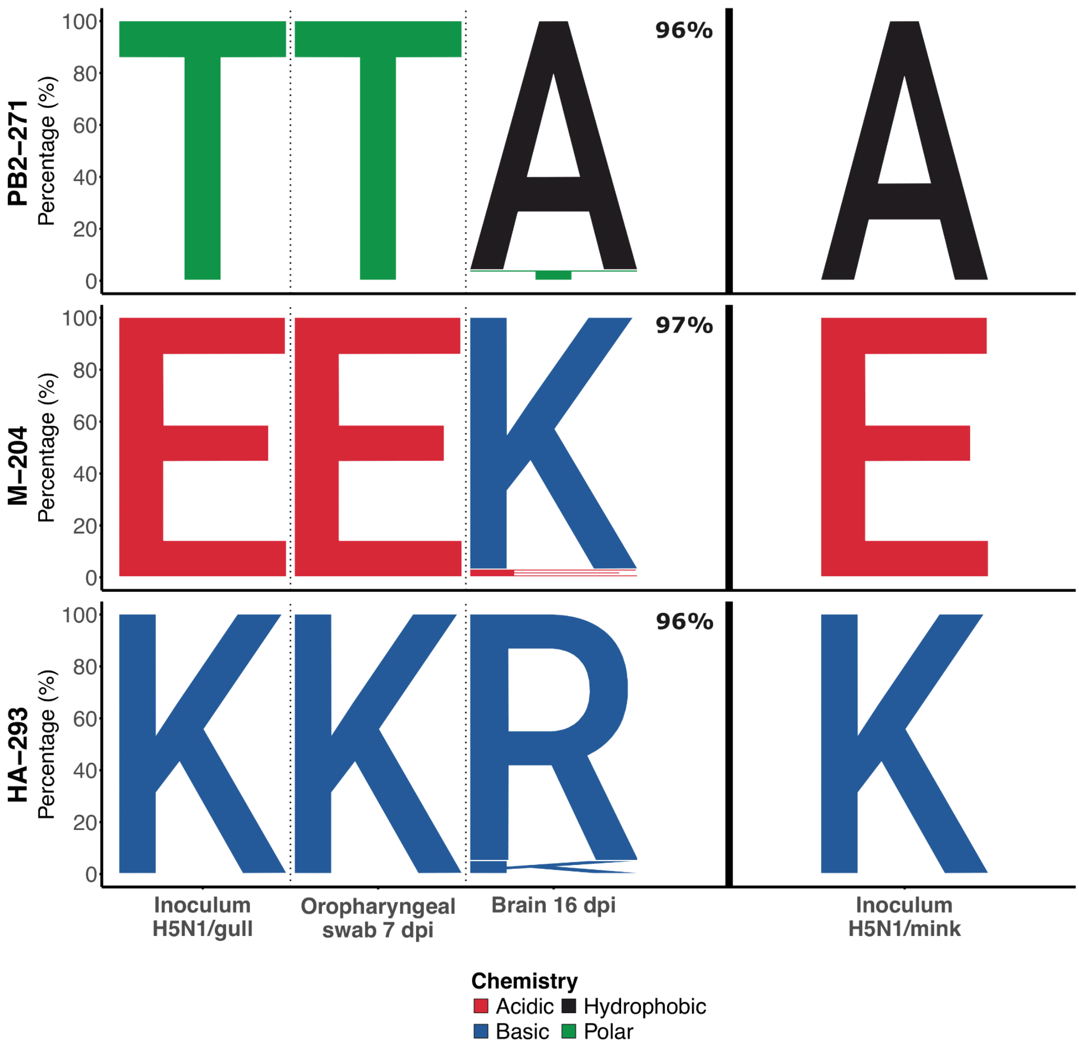

Figure 6. Sequence logos of the relative proportion of amino acids present in the original H5N1/gull inoculum (A/Larus ridibundus/Spain/CR4063/2023), in the virus of the oropharyngeal swab (at 7 dpi) and brain sample (at 16 dpi) of the H5N1/gull-inoculated mink #4 (left), and in the original H5N1/mink inoculum (A/Mink/Spain/3691-8_22VIR10586-10/2022; right), for mutations in the polymerase basic 2 (PB2) protein (position 271), the matrix (M) protein (position 204), and the hemagglutinin (HA) protein (position 293).

Discussion

The current H5N1 clade 2.3.4.4b HPAIV panzootic is being fuelled by bird migratory movements[1], with some outbreaks in farmed and wild mammals being associated with viral circulation in gulls[18,26]. Spillover events occurred across the Americas and Europe, affecting marine mammals, wild and domestic carnivores, dairy cattle, and fur farms[27–30]. These events provide important but limited data on the risk that circulating strains pose at the wildlife-domestic interface, their spillover (bird-to-mammal) and spillback (mammal-to-bird) potential, and their enhanced zoonotic threat[9]. We therefore conducted experimental infections in American minks (*Neogale vison*) and yellow-legged gulls (*Larus michahellis*) using two relevant H5N1 clade 2.3.4.4b HPAIV strains—a mink isolate (H5N1/mink) and a gull isolate (H5N1/gull)—to simulate spillover and spillback events.

We observed high infectivity and pathogenicity when each species was inoculated with a virus originating from the same host (H5N1/gull for gulls and H5N1/mink for minks). However, we did not detect aerosol transmission in any case, and infection by direct contact was only confirmed between gulls. Importantly, efficient gull-to-gull transmission occurred before seeders displayed clinical signs. Considering bird-to-mammal spillover potential, minks inoculated with H5N1/gull had subclinical infection with low viral shedding, but the virus replicated in the central nervous system of two out of four animals with the emergence of a key mammalian adaptation mutation (PB2 T271A). Finally, spillback events seem improbable since gulls inoculated with H5N1/mink virus showed no signs of productive infection.

The avian-adapted H5N1/gull was highly pathogenic in gulls. Both inoculated and direct contact birds developed fatal systemic infections, consistent with global seabird mortality events[31–33] and with European herring gulls (*Larus argentatus*) experimental infections with 2016 H5N8 clade 2.3.4.4b HPAIV[23]. Notably, clinical signs appeared about four days after the onset of viral shedding, suggesting a silent transmission window within colonies. No significant mutations emerged in gulls, indicating low selective pressure in an already adapted host. Similarly, H5N1/mink caused severe disease in inoculated minks, consistent with the associated mink farm outbreak in Spain in October 2022[16]. H5N1/mink showed strong neurotropism, with olfactory and/or haematogenous spread as possible entry pathways[34].

H5N1/gull spread efficiently by direct contact among gulls, suggesting higher dissemination potential of clade 2.3.4.4b viruses compared to previous Gs/GD strains[22,23]. However, we did not confirm aerosol transmission among gulls, but we detected airborne virus in H5N1/gull infected gulls using an active aerosol sampler. We also recorded one positive sample using a passive aerosol sampler, a low-cost tool potentially useful in farms and wetlands.

We failed to observe H5N1/mink direct contact transmission among minks, possibly due to small direct contact groups (two minks per virus), contrasting with the effective mink-to-mink transmission in farm settings with higher animal density (Agüero et al., 2023) or other studies in ferrets[20,35–37]. Additionally, the absence of aerosol transmission among minks is consistent with a previous study with H5N6 clade 2.3.4.4h HPAIV in minks[24], but differs from prior aerosol transmission studies with H5N1 clade 2.3.4.4b in ferrets with mixed results, ranging from absent or limited[25,35,38] to efficient transmission[20,35,39,40]. These inconsistencies may stem from differing hosts, virus strains, or experimental setups.

To simulate a bird-to-mammal spillover event, we exposed American minks to H5N1/gull, mirroring the natural outbreak in farmed minks[16]. While minks lacked clinical signs and mortality, they showed consistent viral shedding and seroconversion, and two out of four individuals (minks #2 and #4) had viral infections in the brain. The involvement of the central nervous system was especially relevant considering that these two individuals had no evidence of systemic infection. As viral RNA was only detected in the oronasal region and in the brain, this might suggest entry via neurons of the olfactory or respiratory epithelia[41], as seen in H5N1/mink infected minks.

Within the brain, H5N1/gull may replicate without systemic immune pressure[42], allowing selection of mammalian-adaptive mutations. At 16 dpi, mink #4 exhibited three such mutations (PB2 T271A, M E204K, and HA K293R) exclusively in the brain, which may have led to the observed weight loss from 7 dpi onwards. While the M E204K and HA K293R variants have not been described, the PB2 T271A is a known adaptation marker that enhances polymerase activity in mammals and whose reversion reduces replication and transmissibility[20]. As this mutation was found in all samples from the 2022 mink outbreak[16] , and as we could now confirm its spontaneous *de novo* emergence after a single exposure, this mutation might play a key role in host adaptation—potentially similar to the spontaneous PB2 E627K amino acid substitution after a single H5N1 HPAIV infection in mice[43]. However, mink #2, which also had a viral infection of the brain, showed no such mutation, indicating variable outcomes in similar conditions. Among minks inoculated with H5N1/mink, one individual developed the PB2 D611N mutation, previously described in mice[44], and another developed the PB2 M645L mutation, which remains uncharacterized. No other adaptive mutations beyond those present in the original H5N1/mink strain were detected.

In contrast to bird-to-mammal spillover events, mammal-to-bird spillback is rare and often inferred phylogenetically, without any experimental infections supporting its presence or frequency[45–47]. We therefore simulated a spillback event by exposing gulls to H5N1/mink, which resulted in no signs of infection even with a high challenge dose. Our findings align with the paucity of natural spillback events and suggest that the potential for a mammalian-adapted H5N1 virus to re-establish in birds is low. However, mammalian isolates that have undergone limited replication and not yet accumulated key adaptive mutations may still retain the ability to infect birds after repeated exposure[40,48]. Notably, despite the high genetic similarity between the two viruses, their phenotypic differences highlight how a few critical mutations can drastically alter host specificity[49].

In summary, our study confirms high mortality of gulls and minks infected with avian- and mammalian-adapted H5N1 clade 2.3.4.4b HPAIVs, respectively, and emphasizes the risk of efficient viral transmission from gulls even before they develop clinical signs, which might pose a significant threat for global seabird populations. While we found no evidence of the mammalian-adapted virus infecting gulls, avian-to-mammal spillover resulted in the infection of minks and a rapidly emerging mammalian adaptation of the virus in the mink CNS as an immunoprivileged environment.

Methods

Viruses

Two clade 2.3.4.4b H5N1 HPAIVs belonging to the EA-2022-BB genotype were used as challenge viruses: i) an avian strain isolated from a gull in Catalonia, Spain in March 2023 (A/Larus ridibundus/Spain/CR4063/2023; EPI_ISL_18983379) (H5N1/gull); and ii) a mammalian strain isolated from an outbreak in a mink farm in Galicia, Spain in October 2022 (A/Mink/Spain/3691-8_22VIR10586-10/2022; EPI_ISL_15878539) (H5N1/mink)[16]. The two viruses share a high degree of nucleotide identity across all gene segments: HA 99.2%, M 97.7%, neuraminidase (NA) 94.5%, NP 98.4%, non-structural protein (NS) 96.5%, polymerase acidic protein (PA) 99.4%, polymerase basic protein 1 (PB1) 99.1%, and PB2 99.6% (Supplementary Data 1). However, H5N1/mink harbours two key mammalian adaptation mutations, PB2 T271A and NA I396M, not present in H5N1/gull, along with other mutations of unknown phenotypic significance[50]. The H5N1/gull virus was propagated and titrated in 10-day-old specific pathogen free embryonated chicken eggs[51]. The H5N1/mink virus (kindly provided by Istituto Zooprofilattico Sperimentale delle Venezie) was produced and titrated in Madin-Darby canine kidney cells without TPCK-trypsin[52].

Experimental infections

All animal procedures were performed at IRTA-CReSA (Catalan Government registration number B9900069) in accordance with the Catalan Government Ethics and Animal Experimentation Committee (CEA-OH/12539/1 and CEA-OH/12238/1 for gulls and minks, respectively), which is subject to national and European regulations (Spanish RD53/2013 and Directive 2010/63/EU). All procedures involving viruses were performed in BSL-3 facilities at IRTA-CReSA with the approval of IRTA's Biosafety Committee (CBS-160-2024 and CBS-150-2024 for gulls and minks, respectively).

The animals were housed in experimental rooms with a negative pressure of 120 Pa, an air filtration rate of 1100 m^3/h, a 12-hour cycle of light and darkness, a constant temperature of 20.5 °C, and 40-60% relative humidity. All animals (gulls and minks) tested negative for both viral RNA detection via RT-qPCR and anti-NP antibodies by competitive ELISA (ID Screen) before challenge.

Gulls

Forty yellow-legged gulls (*Larus michahellis*) were captured in May 2024 as part of the nest elimination campaign during hatching season at 1-2 weeks post-hatch at the natural reserve Punta de la Banya, Parc Natural del Delta de l'Ebre, La Ràpita, Catalonia, Spain (capture permit FUE-2024-03756074). Upon capture, birds were transferred to the animal BSL-3 facilities of IRTA-CReSA where they underwent a 1-month acclimation period. Gulls were fed every 2-3 h the first week upon arrival, 3-4 times a day the second and third weeks, and twice a day after that with a 1:1 mixture of wet cat food and fresh fish (sardines and anchovies). Food was supplemented with calcium carbonate (NEKTON Calcium-Plus, Nekton) and a multi-vitamin B mix (NEKTON-Biotin, Nekton) during the first two weeks.

Each of the two experimental rooms (one per viral strain) was physically separated in 3 areas (Supplementary Figure 1A): a) inoculated (n=10) and direct contacts (n=4); b) buffer area (1 m width x 1 m height); and c) aerosol contacts (n=4).

At 4-6 weeks of age, gulls in the inoculated groups were inoculated with 10^5 mean embryo infectious doses (EID_{50}) of H5N1/gull (n=10) or 10^5 mean tissue culture infectious doses ($TCID_{50}$) of H5N1/mink (n=10). The final volume of the inoculum was 100 μl, of which

50 µl were inoculated intranasally and 50 µl intrachoanally. The inocula were back titrated on the day of inoculation and confirmed to be 10^5 EID_{50} for the H5N1/gull virus and 10^5 $TCID_{50}$ for the H5N1/mink virus. Twenty-four hours post-inoculation, direct contacts (n=4/virus) and aerosol contacts (n=4/virus) were added in the corresponding experimental room areas. Birds were monitored daily for clinical signs and mortality until 14 dpi [53,54]. Severely sick birds were euthanised by intravenous overdose of sodium pentobarbital (140 mg/kg) under intramuscular anaesthesia with ketamine (10 mg/kg) and xylazine (1 mg/kg) and counted as dead on that day in the MDT calculations. At 14 dpi, the surviving birds were bled to collect serum samples and euthanised.

To investigate individual viral shedding, oropharyngeal swabs, cloacal swabs, and feather pulp samples from the breast skin were collected from all birds at 2, 4, 7, 10, and 14 dpi. These samples were preserved in 1 ml phosphate-buffered saline (PBS) with 1% penicillin/streptomycin (P/S). Whole blood in tubes with EDTA were collected at 7 and 14 dpi, or from gulls euthanised for ethical reasons.

To examine for gross lesions and collect tissues for histological evaluation in the asymptomatic phase of infection, three inoculated gulls from each challenge virus group were euthanised and necropsied at 3 dpi. To evaluate severe and morbid phases of infection, up to three gulls per challenge virus and condition (inoculated, direct contacts, and aerosol contacts) found dead or ethically euthanised were necropsied and tissues collected. For reference, two negative controls from each experimental room were euthanised and necropsied pre-challenge. A complete set of tissues were collected in 10% neutral buffered formalin for histopathological examination. For viral RNA detection, sections of the brain, lung, spleen, and heart were collected in Dulbecco's Modified Eagle Medium (DMEM) + 1% P/S with a 5 mm-stainless steel bead (QIAGEN).

To evaluate viral contamination in the environment, aerosol and drinking water samples were collected at 2, 4, 7, 10, and 14 dpi. Aerosol sampling was performed using two different strategies: i) active sampling with a Coriolis μ Air sampler (Bertin Technologies) set for 2 h with a 100 L/min flow rate input; and ii) passive sampling using Modified Wilson and Cooke samplers[55], which we built in-house and filled with 100 μL of sterile PBS. Both devices were placed in the buffer area (Supplementary Figures 1B-C). Drinking water was sampled using 5 mL Falcon tubes and was changed daily after sampling.

Minks

Thirty-six minks 10-18 months-old (*Neogale vison*) were purchased in a mink farm in Spain (50% females). Animals had *ad libitum* access to food and water with a combination of solid and wet cat food. Minks were acclimated for 10 days before inoculation and housed in 11000 cm^2 F-suite cages (Tecniplast), containing 2-3 animals per cage. Each of the two experimental rooms (one per virus) had 6 F-suite cages containing a total of 18 animals and divided in four groups (Supplementary Figure 2A): negative controls (n=3), inoculated (n=7), direct contacts (n=2), and aerosol contacts (n=6). In this setting, there were two cage pairs composed of one inoculated/direct contact cage and one aerosol contact cage each, separated by 40 cm and two metal grids (0.1 cm^2). Each cage had two 5500 cm^2 levels connected by a tube (Supplementary Figure 2B).

Minks in the inoculated groups were sedated with a combination of butorphanol (0.5 mg/kg), midazolam (0.5 mg/kg), and medetomidine (0.01 mg/kg) intramuscularly, and then intranasally inoculated with 10^5 $TCID_{50}$/animal of H5N1/mink or H5N1/gull. The final volume of the inoculum was 200 μl. The inocula were back titrated on the day of inoculation and confirmed to be 10^5 EID_{50} for the H5N1/gull virus and 10^5 $TCID_{50}$ for the H5N1/mink virus. Direct contact and aerosol contact minks were already allocated in their corresponding cages upon inoculation. After inoculation, minks were supervised daily following a detailed scoring system adapted from ferrets[56]. At 2, 4, 7, 9, 11, and 14 dpi body weight, rectal temperature, and ocular and nasal secretions were recorded under sedation (butorphanol and midazolam, 0.5 mg/kg each). At these same time points, oropharyngeal swabs were also collected in 1 ml DMEM with 1% P/S to evaluate viral shedding. Whole blood and serum samples were collected at 7 dpi and experimental endpoint (14 dpi for H5N1/mink and 16 dpi for H5N1/gull), or from minks euthanised for ethical reasons (HEP). Minks were euthanised at experimental endpoint or at HEP if they reached a 20% weight loss or presented moderate signs of CNS infection. Minks were euthanised under sedation by intravenous sodium pentobarbital (120mg/kg) and counted as dead on that day in the MDT calculations.

Negative controls (n=2-3) from each experimental room were euthanised and necropsied pre-challenge as reference. To examine for gross lesions and collect tissues for histological evaluation during the acute phase of infection, three inoculated minks from each challenge virus group were euthanised and necropsied at 3 dpi. All surviving minks were euthanised and necropsied at experimental endpoint. A complete set of tissues were collected in 10% neutral buffered formalin for histopathological examination. For viral RNA detection, fragments of the caudal lung and the temporal lobe were collected in DMEM + 2% P/S with a 5 mm-stainless steel bead (QIAGEN).

Environmental sampling was performed at 2, 4, 7, 9, 11, and 14 dpi using a Coriolis μ Air sampler (Bertin Technologies). The equipment was placed in a corner below the exhaust (Supplementary Figure 2C), and it was set for 2 h with a flow rate input of 100 L/min. A reservoir filled with distilled water was also placed to compensate for evaporation at a pace of 0.1 mL/min.

Viral RNA quantification

Prior to viral extraction from passive and active aerosol environmental samples, a concentration step was performed using Amicon Ultra-15 10 kDa centrifugal filter units (Sigma-Aldrich), following the manufacturer's protocol. The concentrated fraction (200 µL) was inactivated in VXL lysis buffer. Water samples were not concentrated by centrifugal filters to optimize virus yield.

Tissues collected for virological analysis (gulls: lung, brain, heart, and spleen; minks: lung and brain) were homogenised at 30 Hz for 1 min with a TissueLyser II (QIAGEN) and centrifuged for 10 min at 10,000 rpm at 4 C. The supernatant was collected in VXL lysis buffer. Mink oropharyngeal swabs and gull oropharyngeal and cloacal swabs and feather pulp samples were also collected in VXL lysis buffer. Whole blood (200 µL) was also inactivated in VXL buffer. All samples were frozen at -80 °C until extraction was performed. RNA was extracted using the IndiMag Pathogen Kit (Indical) on a Biosprint 96 workstation (QIAGEN).

Viral RNA detection was performed via RT-qPCR by targeting a highly conserved region of the influenza matrix 1 (M1) gene with a one-step Taqman RT–PCR in a Fast7500 equipment (Applied Biosystems), using primers and probes described elsewhere[57].

Histopathology and viral in situ detection

For histopathology, tissue sections were fixed in 10% neutral buffered formalin, paraffin-embedded, and sectioned at 3 µm. Prior to paraffin-embedding, nasal cavity tissues were decalcified in 0.27 M pH 7.4 EDTA solution until softening. Slides were stained with hematoxylin and eosin (HE) and examined by light microscopy. Slides were additionally scanned at x20 using Olympus VS200 Slide Scanner. For viral tissue distribution, serial 3 µm-sections were obtained from formalin-fixed paraffin-embedded tissues, mounted on charged slides and stained with immunohistochemistry (IHC)[58]. To investigate viral tissue replication at 3 dpi (gulls) and at early and late stage of infection (minks), RNAscope in situ hybridization (ISH) assay was additionally performed on selected tissues (i.e., lung from gulls; nasal cavity and brain from minks) using a custom-designed probe (V-H5N8-M1M2) targeting the influenza M1 and M2 protein genes of H5 clade 2.3.4.4b HPAIV and using the RNAscope® 2.5 HD Assay RED following manufacturer's recommendations (Advanced Cell Diagnostics)[59]. A probe targeting the dihydrodipicolinate reductase gene from the *Bacillus subtilis* strain SMY was used as a negative control, while sections of AIV positive tissues were used as positive controls.

Serology

Sera from all animals before challenge, at 7 dpi, euthanised at HEP, and euthanised at experimental endpoint (14 dpi for gulls and H5N1/mink infected minks, and 16 dpi for H5N1/gull infected minks) were tested by a commercial competitive ELISA against NP to evaluate seroconversion following the manufacturers' specifications.

Nanopore genomics

Nanopore sequencing of RNA extracts was performed on a subset of samples to investigate viral adaptation through low-frequency variant analysis. Both inocula (H5N1/mink and H5N1/gull) were sequenced. From the gull experiment using the H5N1/gull virus, oropharyngeal swabs collected at 10 dpi were sequenced from three inoculated birds (gulls #2B, #3B, and #4B) and three direct contacts (gulls #1Y, #3Y, and #4Y). From the mink experiment using the H5N1/mink virus, oropharyngeal swabs collected at 4 dpi were sequenced from three inoculated animals (minks #19, #20, and #23). Finally, in the mink experiment using the H5N1/gull virus, oropharyngeal swabs (collected at 7 dpi) and brain samples (collected at 16 dpi) were sequenced from two inoculated animals (minks #2 and #4).

All RNA samples were subjected to cDNA conversion, and multi-segment amplification using M-RTPCR as previously described[60]. Briefly, the RNA was mixed with SuperScript III One-Step PCR (Invitrogen) buffer and enzyme mix (containing the reverse transcriptase enzyme and the PCR amplification enzyme). The thermal cycle parameters were 42 °C for 60 min, 94 °C for 2 min, and then 5 cycles (94 °C for 30 s, 45 °C for 30 s, and 68 °C for 3 min), followed by 31 cycles (94 °C for 30 s, 57 °C for 30 s, and 68 °C for 3 min). Primers used were MBTuni-12 (5′-ACGCGTGATCAGCAAAAGCAGG) and MBTuni-13 (5′-ACGCGTGATCAGTAGAAACAAGG) that correspond to the 5′ and 3′ conserved sequences of all eight influenza A segments, and that have been demonstrated effective on all subtypes. Sequencing was then performed using a portable MinION Mk1C device and a FLO-MIN114 R10.4.1 flow cell (Oxford Nanopore Technologies), following our previously established protocol for AIV surveillance using the rapid barcoding library preparation (SQK-RBK114.24)[61].

For nanopore raw data processing, POD5 files were basecalled using the SUP accuracy model in Dorado (v0.9.1; https://github.com/nanoporetech/dorado), which also removed sequencing primers and adapters. Quality filtering of reads (minimum Phred score >8) and length filtering (>150 bp) were performed using Filtlong (v0.2.1; https://github.com/rrwick/Filtlong). The resulting FASTQ files were aligned to the reference genomes using Minimap2 (v2.26) with the -ax map-ont setting[62]. The reference sequences used were GISAID accession numbers EPI_ISL_15878539 (H5N1/mink) and EPI_ISL_18983379 (H5N1/gull). The resulting SAM files were converted to BAM format, sorted, and indexed using SAMtools (v1.17)[63], and genome coverage distributions were obtained. Variant calling was then performed with Clair3 (v1.0.9;

https://github.com/HKU-BAL/Clair3), using --snp_min_af=0.01 and --indel_min_af=0.01 to detect low-frequency variants. Identified variants were annotated with SnpEff (v5.2f)[64] to determine the resulting amino acid changes. Variants from animal samples were compared with those from the inoculum. Only variants that were either unique to the animal samples or showed a frequency difference of ≥25% between the inoculum and the animal samples were retained. Additionally, a stringent criterion of a minimum depth coverage of 100x per variant and a minimum variant frequency of 5% in the animal sample was applied to reduce false positives. The accepted variants were analyzed with Flumut (v0.6.4)[65] to determine whether previous studies had analyzed the phenotypic changes of the variants.

Statistical analyses

Statistical analyses were performed using GraphPad (v10.4.1; GraphPad Prism). Multiple comparisons between inoculated, direct contact and aerosol contact gulls in the H5N1/gull room were conducted using the non-parametric Kruskal-Wallis test with Dunn's correction for multiple comparisons. Comparisons between H5N1/mink- and H5N1/gull-inoculated minks were performed using the non-parametric Mann-Whitney unpaired U test. Survival data from Kaplan-Meier curves were analysed using the Mantel-Cox test. A two-sided *p-value* below 0.05 was considered statistically significant.

Data availability

Original fastq files from all the sequencing runs are available at ENA PRJEB95805 accession study. All our computational scripts are available via the GitHub repository: *https://github.com/Albertperlas/From_feather_to_fur*. All other data supporting the findings of this study are available within the article, its Supplementary Information, or from the corresponding authors upon reasonable request.

References

1. Klaassen, M. & Wille, M. The plight and role of wild birds in the current bird flu panzootic. *Nat Ecol Evol* **7**, 1541–1542 (2023).
2. Webster, R. G., Bean, W. J., Gorman, O. T., Chambers, T. M. & Kawaoka, Y. Evolution and ecology of influenza A viruses. *Microbiol Rev* **56**, 152–179 (1992).
3. Gass, J. D. *et al.* Global dissemination of Influenza A virus is driven by wild bird migration through arctic and subarctic zones. *Mol Ecol* **32**, 198–213 (2023).
4. J, R. & W, G. The economics of animal health: direct and indirect costs of animal disease outbreaks. 18 p. (2016) doi:10.20506/TT.2551.
5. Suarez, D. L. Influenza A virus. in *Animal Influenza* 1–30 (John Wiley & Sons, Ltd, 2016). doi:10.1002/9781118924341.ch1.
6. Xu, X., Subbarao, null, Cox, N. J. & Guo, Y. Genetic characterization of the pathogenic influenza A/Goose/Guangdong/1/96 (H5N1) virus: similarity of its hemagglutinin gene to those of H5N1 viruses from the 1997 outbreaks in Hong Kong. *Virology* **261**, 15–19 (1999).
7. Shi, J., Zeng, X., Cui, P., Yan, C. & Chen, H. Alarming situation of emerging H5 and H7 avian influenza and effective control strategies. *Emerg Microbes Infect* **12**, 2155072 (2023).
8. Lowen, A. C. *et al.* Controlling bird flu is urgent—for dairy, wildlife, poultry, pets, and people. (2025) doi:10.2460/javma.25.05.0294.

9. Bellido-Martín, B. *et al.* Evolution, spread and impact of highly pathogenic H5 avian influenza A viruses. *Nat Rev Microbiol* 1–16 (2025) doi:10.1038/s41579-025-01189-4.

10. Krammer, F., Hermann, E. & Rasmussen, A. L. Highly pathogenic avian influenza H5N1: history, current situation, and outlook. *J Virol* **99**, e0220924 (2025).

11. Authority, E. F. S. *et al.* Avian influenza overview December 2024–March 2025. *EFSA Journal* **23**, e9352 (2025).

12. Peacock, T. P. *et al.* The global H5N1 influenza panzootic in mammals. *Nature* **637**, 304–313 (2025).

13. Fusaro, A. *et al.* High pathogenic avian influenza A(H5) viruses of clade 2.3.4.4b in Europe – why trends of virus evolution are more difficult to predict. *Virus Evolution* veae027 (2024) doi:10.1093/ve/veae027.

14. Ramey, A. M. *et al.* Highly pathogenic avian influenza is an emerging disease threat to wild birds in North America. *The Journal of Wildlife Management* **86**, (2022).

15. Adlhoch, C. *et al.* Avian influenza overview September – December 2022. *EFSA Journal* **21**, 7786 (2023).

16. Agüero, M. *et al.* Highly pathogenic avian influenza A(H5N1) virus infection in farmed minks, Spain, October 2022. *Eurosurveillance* **28**, (2023).

17. Bessière, P. *et al.* Cats as sentinels of mammal exposure to H5Nx avian influenza viruses: a seroprevalence study, France, December 2023 to January 2025. *Eurosurveillance* **30**, 2500189 (2025).

18. Kareinen, L. *et al.* Highly pathogenic avian influenza A(H5N1) virus infections on fur farms connected to mass mortalities of black-headed gulls, Finland, July to October 2023. *Eurosurveillance* **29**, 2400063 (2024).

19. Nguyen, T.-Q. *et al.* Emergence and interstate spread of highly pathogenic avian influenza A(H5N1) in dairy cattle in the United States. *Science* **388**, eadq0900 (2025).

20. Restori, K. H. *et al.* Risk assessment of a highly pathogenic H5N1 influenza virus from mink. *Nat Commun* **15**, 4112 (2024).

21. Global AIV with Zoonotic Potential. *AnimalHealth* https://www.fao.org/animal-health/situation-updates/global-aiv-with-zoonotic-potential/en.

22. Gulyaeva, M. A., Sharshov, K. A., Zaykovskaia, A. V., Shestopalova, L. V. & Shestopalov, A. M. Experimental infection and pathology of clade 2.2 H5N1 virus in gulls. *Journal of Veterinary Science* **17**, 179–188 (2016).

23. Tarasiuk, K. *et al.* Pathogenicity of highly pathogenic avian influenza H5N8 subtype for herring gulls (Larus argentatus): impact of homo- and heterosubtypic immunity on the outcome of infection. *Veterinary research* **53**, 108 (2022).

24. Sun, H. *et al.* Mink is a highly susceptible host species to circulating human and avian influenza viruses. *Emerging Microbes and Infections* **10**, 472–480 (2021).

25. Maemura, T. *et al.* Characterization of highly pathogenic clade 2.3.4.4b H5N1 mink influenza viruses. *eBioMedicine* **97**, (2023).

26. Uhart, M. M. *et al.* Epidemiological data of an influenza A/H5N1 outbreak in elephant seals in Argentina indicates mammal-to-mammal transmission. *Nat Commun* **15**, 9516 (2024).

27. Kareinen, L. *et al.* Highly pathogenic avian influenza A(H5N1) virus infections on fur farms connected to mass mortalities of black-headed gulls, Finland, July to October 2023. *Eurosurveillance* **29**, 2400063 (2024).

28. Caserta, L. C. *et al.* Spillover of highly pathogenic avian influenza H5N1 virus to dairy cattle. *Nature* **634**, 669–676 (2024).

29. Chestakova, I. V. *et al.* High number of HPAI H5 virus infections and antibodies in wild carnivores in the Netherlands, 2020–2022. *Emerging Microbes & Infections* **12**, 2270068 (2023).
30. Rimondi, A. *et al.* Highly Pathogenic Avian Influenza A(H5N1) Viruses from Multispecies Outbreak, Argentina, August 2023 - Volume 30, Number 4—April 2024 - Emerging Infectious Diseases journal - CDC. doi:10.3201/eid3004.231725.
31. Leguia, M. *et al.* Highly pathogenic avian influenza A (H5N1) in marine mammals and seabirds in Peru. *Nat Commun* **14**, 5489 (2023).
32. Pohlmann, A. *et al.* Mass mortality among colony-breeding seabirds in the German Wadden Sea in 2022 due to distinct genotypes of HPAIV H5N1 clade 2.3.4.4b. *Journal of General Virology* **104**, 001834 (2023).
33. McPhail, G. M. *et al.* Geographic, ecological, and temporal patterns of seabird mortality during the 2022 HPAI H5N1 outbreak on the island of Newfoundland. *Can. J. Zool.* **103**, 1–12 (2025).
34. Schrauwen, E. J. A. *et al.* The multibasic cleavage site in H5N1 virus is critical for systemic spread along the olfactory and hematogenous routes in ferrets. *Journal of virology* **86**, 3975–84 (2012).
35. Pulit-Penaloza, J. A. *et al.* Transmission of a human isolate of clade 2.3.4.4b A(H5N1) virus in ferrets. *Nature* **636**, 705–710 (2024).
36. Tosheva, I. I. *et al.* Influenza A(H5N1) shedding in air corresponds to transmissibility in mammals. *Nat Microbiol* **10**, 14–19 (2025).
37. Kobasa, D. *et al.* Transmission of lethal H5N1 clade 2.3.4.4b avian influenza in ferrets. Preprint at https://doi.org/10.21203/rs.3.rs-2842567/v1 (2023).
38. Eisfeld, A. J. *et al.* Pathogenicity and transmissibility of bovine H5N1 influenza virus. *Nature* **633**, 426–432 (2024).

39. Gu, C. *et al.* A human isolate of bovine H5N1 is transmissible and lethal in animal models. *Nature* **636**, 711–718 (2024).
40. Marchenko, V. Yu. *et al.* Characterization of H5N1 avian influenza virus isolated from bird in Russia with the E627K mutation in the PB2 protein. *Sci Rep* **14**, 26490 (2024).
41. Bauer, L., Benavides, F. F. W., Veldhuis Kroeze, E. J. B., de Wit, E. & van Riel, D. The neuropathogenesis of highly pathogenic avian influenza H5Nx viruses in mammalian species including humans. *Trends in Neurosciences* **46**, 953–970 (2023).
42. Cele, S. *et al.* SARS-CoV-2 prolonged infection during advanced HIV disease evolves extensive immune escape. *Cell Host Microbe* **30**, 154-162.e5 (2022).
43. Kim, D.-H., Lee, D.-Y., Seo, Y., Song, C.-S. & Lee, D.-H. Immediate PB2-E627K amino acid substitution after single infection of highly pathogenic avian influenza H5N1 clade 2.3.4.4b in mice. *Virology Journal* **22**, 183 (2025).
44. Qi, L. *et al.* Analysis by Single-Gene Reassortment Demonstrates that the 1918 Influenza Virus Is Functionally Compatible with a Low-Pathogenicity Avian Influenza Virus in Mice. *Journal of Virology* **86**, 9211–9220 (2012).
45. Pardo-Roa, C. *et al.* Cross-species and mammal-to-mammal transmission of clade 2.3.4.4b highly pathogenic avian influenza A/H5N1 with PB2 adaptations. *Nat Commun* **16**, 2232 (2025).
46. Rimondi, A. *et al.* Highly Pathogenic Avian Influenza A(H5N1) Viruses from Multispecies Outbreak, Argentina, August 2023 - Volume 30, Number 4—April 2024 - Emerging Infectious Diseases journal - CDC. doi:10.3201/eid3004.231725.
47. Tomás, G. *et al.* Highly pathogenic avian influenza H5N1 virus infections in pinnipeds and seabirds in Uruguay: Implications for bird–mammal transmission in South America. *Virus Evol* **10**, veae031 (2024).

48. Authority, E. F. S. *et al.* Avian influenza overview March–June 2024. *EFSA Journal* **22**, e8930 (2024).
49. Lin, T.-H. *et al.* A single mutation in bovine influenza H5N1 hemagglutinin switches specificity to human receptors. *Science* **386**, 1128–1134 (2024).
50. Agüero, M. *et al.* Authors' response: Highly pathogenic influenza A(H5N1) viruses in farmed mink outbreak contain a disrupted second sialic acid binding site in neuraminidase, similar to human influenza A viruses. *Eurosurveillance* **28**, 2300109 (2023).
51. Spackman, E. & Killian, M. L. Avian Influenza Virus Isolation, Propagation, and Titration in Embryonated Chicken Eggs. in *Animal Influenza Virus: Methods and Protocols* (ed. Spackman, E.) 149–164 (Springer US, New York, NY, 2020). doi:10.1007/978-1-0716-0346-8_12.
52. Zhang, J. & Gauger, P. C. Isolation of Swine Influenza A Virus in Cell Cultures and Embryonated Chicken Eggs. *Methods Mol Biol* **2123**, 281–294 (2020).
53. World Organisation for Animal Health (WOAH). *Avian Influenza (Including Infection with High Pathogenicity Avian Influenza Viruses) WOAH Terrestrial Manual 2021*. (World Organisation for Animal Health, Paris, France, 2021).
54. Filaire, F. *et al.* Viral shedding and environmental dispersion of two clade 2.3.4.4b H5 high pathogenicity avian influenza viruses in experimentally infected mule ducks: implications for environmental sampling. *Veterinary Research* **55**, 100 (2024).
55. Webb, N. *et al. Standard Methods for Wind Erosion Research and Model Development: Protocol for the National Wind Erosion Research Network*. (2015).
56. Martínez-Orellana, P. *et al.* Clinical response to pandemic h1n1 influenza virus from a fatal and mild case in ferrets. *Virology Journal* **12**, 48 (2015).

57. Heine, H. G., Trinidad, L., Selleck, P. & Lowther, S. Rapid Detection of Highly Pathogenic Avian Influenza H5N1 Virus by TaqMan Reverse Transcriptase–Polymerase Chain Reaction. *avdi* **51**, 370–372 (2007).

58. Gaide, N. *et al.* The feather epithelium contributes to the dissemination and ecology of clade 2.3.4.4b H5 high pathogenicity avian influenza viruses in ducks. *Emerg Microbes Infect* **12**, 2272644 (2023).

59. Gaide, N. *et al.* Validation of an RNAscope assay for the detection of avian influenza A virus. *J Vet Diagn Invest* **35**, 500–506 (2023).

60. Zhou, B. *et al.* Single-Reaction Genomic Amplification Accelerates Sequencing and Vaccine Production for Classical and Swine Origin Human Influenza A Viruses. *Journal of Virology* **83**, 10309–10313 (2009).

61. Perlas, A. *et al.* Improvements in RNA and DNA nanopore sequencing allow for rapid genetic characterization of avian influenza. *Virus Evolution* veaf010 (2025) doi:10.1093/ve/veaf010.

62. Li, H. Minimap2: pairwise alignment for nucleotide sequences. *Bioinformatics* **34**, 3094–3100 (2018).

63. Li, H. *et al.* The Sequence Alignment/Map format and SAMtools. *Bioinformatics* **25**, 2078–2079 (2009).

64. Cingolani, P. *et al.* A program for annotating and predicting the effects of single nucleotide polymorphisms, SnpEff: SNPs in the genome of Drosophila melanogaster strain w1118; iso-2; iso-3. *Fly* **6**, 80–92 (2012).

65. Giussani, E. *et al.* FluMut: a tool for mutation surveillance in highly pathogenic H5N1 genomes. *Virus Evol* **11**, veaf011 (2025).

Acknowledgements

This work was supported by the Wildflu project under the ISIDORe Trans-National Access (TNA) programme (project ID ISID_4642), funded by the European Union's Horizon Europe Research and Innovation programme (grant agreement No. 101046133). K.B. is funded by the Ministry of Economy and Competitiveness, Spain, program Ramón y Cajal (Grant RYC2021-033472-I). The H5N1 clade 2.3.4.4b HPAIV A/Mink/Spain/3691-8_22VIR10586-10/2022 was kindly provided by Istituto Zooprofilattico Sperimentale delle Venezie. We acknowledge the use of ChatGPT (GPT-4 and GPT-5, OpenAI) for assistance in language refinement and providing support in code development. All content and code were reviewed and verified by the authors.

Author contributions

A.P., F.T.-F. and K.B. designed the study, planned and supervised the experimental infections, and wrote the manuscript; P.B. and N.G. assisted with experimental work, processed samples for histopathology and contributed to manuscript preparation; L.M., E.C., J.M., M.N., R.V., A.G., Ma.P., Mo.P., M.J.V.-M. and I.C. performed animal experiments, sample collection, laboratory analyses, and data interpretation; T.R. implemented bioinformatic workflows and scripts for influenza sequencing and data interpretation; A.P., F.T.-F., N.G., N.M., J.-L.G., L.U. and K.B. contributed to project conceptualisation and funding acquisition, with A.P. as principal investigator; N.M., J.-L.G., L.U. and K.B. provided senior supervision and guidance with substantial contribution to the manuscript; all authors reviewed and approved the final manuscript.

Competing interests

The authors declare no competing interests.

Supplementary Files

This is a list of supplementary files associated with this preprint. Click to download.

- Additionalinformation.pdf